

Emission polarization control in semiconductor quantum dots coupled to a photonic crystal microcavity

E. Gallardo,^{1,*} L. J. Martínez,² A. K. Nowak,¹ H. P. van der Meulen,¹ J. M. Calleja,¹ C. Tejedor,¹ I. Prieto,² D. Granados,² A. G. Taboada,² J. M. García,² and P. A. Postigo²

¹Departamento de Física de Materiales, Universidad Autónoma de Madrid, E-28049 Madrid, Spain

²Instituto de Microelectrónica de Madrid, Centro Nacional de Microelectrónica, Consejo Superior de Investigaciones Científicas, Isaac Newton 8, PTM Tres Cantos, E-28760 Madrid, Spain

*eva.gallardo@uam.es

Abstract: We study the optical emission of single semiconductor quantum dots weakly coupled to a photonic-crystal micro-cavity. The linearly polarized emission of a selected quantum dot changes continuously its polarization angle, from nearly perpendicular to the cavity mode polarization at large detuning, to parallel at zero detuning, and reversing sign for negative detuning. The linear polarization rotation is qualitatively interpreted in terms of the detuning dependent mixing of the quantum dot and cavity states. The present result is relevant to achieve continuous control of the linear polarization in single photon emitters.

©2010 Optical Society of America

OCIS codes: (160.4760) Optical properties; (230.5298) Photonic crystals; (230.5590) Quantum-well, -wire and -dot devices.

References and links

1. P. Michler, A. Kiraz, C. Becher, W. V. Schoenfeld, P. M. Petroff, L. Zhang, E. Hu, and A. Imamoglu, "A quantum dot single photon source," *Adv. Solid State Phys.* **41**, 3–14 (2001) (and references therein).
2. K. J. Vahala, "Optical microcavities," *Nature* **424**(6950), 839–846 (2003) (and references therein).
3. E. M. Purcell, "Spontaneous emission probabilities at radio frequencies," *Phys. Rev.* **69**, 681 (1946).
4. J. P. Reithmaier, G. Sek, A. Löffler, C. Hofmann, S. Kuhn, S. Reitzenstein, L. V. Keldysh, V. D. Kulakovskii, T. L. Reinecke, and A. Forchel, "Strong coupling in a single quantum dot-semiconductor microcavity system," *Nature* **432**(7014), 197–200 (2004).
5. T. Yoshie, A. Scherer, J. Hendrickson, G. Khitrova, H. M. Gibbs, G. Rupper, C. Ell, O. B. Shchekin, and D. G. Deppe, "Vacuum Rabi splitting with a single quantum dot in a photonic crystal nanocavity," *Nature* **432**(7014), 200–203 (2004).
6. N. Akopian, N. H. Lindner, E. Poem, Y. Berlatzky, J. Avron, D. Gershoni, B. D. Gerardot, and P. M. Petroff, "Entangled photon pairs from semiconductor quantum dots," *Phys. Rev. Lett.* **96**(13), 130501 (2006).
7. R. M. Stevenson, R. J. Young, P. Atkinson, K. Cooper, D. A. Ritchie, and A. J. Shields, "A semiconductor source of triggered entangled photon pairs," *Nature* **439**(7073), 179–182 (2006).
8. A. Daraei, D. Sanvitto, J. A. Timpson, A. M. Fox, D. M. Whittaker, M. S. Skolnick, P. S. S. Guimarães, H. Vinck, A. Tahaoui, P. W. Fry, S. L. Liew, and M. Hopkinson, "Control of polarization and mode mapping of small volume high Q micropillars," *J. Appl. Phys.* **102**(4), 043105 (2007).
9. R. Oulton, B. D. Jones, S. Lam, A. R. A. Chalcraft, D. Szymanski, D. O'Brien, T. F. Krauss, D. Sanvitto, A. M. Fox, D. M. Whittaker, M. Hopkinson, and M. S. Skolnick, "Polarized quantum dot emission from photonic crystal nanocavities studied under moderate resonant enhanced excitation," *Opt. Express* **15**(25), 17221–17230 (2007).
10. D. Granados, and J. M. García, "In(Ga)As self-assembled quantum ring formation by molecular beam epitaxy," *Appl. Phys. Lett.* **82**(15), 2401 (2003).
11. B. Alén, J. Martínez-Pastor, D. Granados, and J. M. García, "Continuum and discrete excitation spectrum of single quantum rings," *Phys. Rev. B* **72**(15), 155331 (2005).
12. N. A. J. M. Kleemans, I. M. A. Bomiñaar-Silkens, V. M. Fomin, V. N. Gladilin, D. Granados, A. G. Taboada, J. M. García, P. Offermans, U. Zeitler, P. C. M. Christianen, J. C. Maan, J. T. Devreese, and P. M. Koenraad, "Oscillatory persistent currents in self-assembled quantum rings," *Phys. Rev. Lett.* **99**(14), 146808 (2007).
13. K. Hennessy, A. Badolato, P. M. Petroff, and E. Hu, "Positioning photonic crystal cavities to single InAs quantum dots," *Photon. Nanostruct.—Fundam. Appl.* **2**(2), 65–72 (2004).
14. K. Hennessy, C. Högerle, E. Hu, A. Badolato, and A. Imamoglu, "Tuning photonic nanocavities by atomic force microscope nano-oxidation," *Appl. Phys. Lett.* **89**(4), 041118 (2006).

15. S. Mosor, J. Hendrickson, B. C. Richards, J. Sweet, G. Khitrova, H. M. Gibbs, T. Yoshie, A. Scherer, O. B. Shchekin, and D. G. Deppe, "Scanning a photonic crystal slab nanocavity by condensation of xenon," Appl. Phys. Lett. **87**(14), 141105 (2005).
 16. P. Offermans, P. M. Koenraad, J. H. Wolter, D. Granados, J. M. García, V. M. Fomin, V. N. Gladilin, and J. T. Devreese, "Atomic-scale structure of self-assembled In(Ga)As quantum rings in GaAs," Appl. Phys. Lett. **87**(13), 131902 (2005).
-

1. Introduction

Semiconductor quantum dots (QDs) coupled to optical microcavities are at the basis of efficient single photon emitters (SPEs) for quantum information applications [1,2]. Depending on the cavity design and the QD location, a significant enhancement of the spontaneous emission rate (Purcell effect) [3] is obtained in the weak coupling regime. For strong coupling, entangled light-matter states appear that can be used as building blocks for quantum information treatment [4,5]. Continuous control of the linearly polarized emission of QDs is desirable to obtain variable polarization SPEs and controlled sources of entangled photon pairs [6,7]. The polarization of the photons emitted by a single QD is known to be influenced by its coupling to an optical micro-cavity mode (CM) [8,9]. In QDs embedded in a micropillar cavity with elliptical cross section [8] the polarization of the light emitted at the QD energy becomes parallel to that of the CM closest in energy. Also QDs coupled to a photonic crystal microcavity (PCM) [9] are reported to maintain their polarization parallel to the CM even for large energy difference (detuning, Δ) between the emission of the QD and the CM. Both systems present an important difference: while the QD-photons of micropillar cavities are mainly emitted along their axis (the usual collection direction) and cavity-photons are mainly emitted perpendicular to it, PCMs emit both cavity- and QD-photons in the same direction.

In this article we present measurements of the emission polarization angle (Φ) of two QDs weakly coupled to a H1 (calzone) PCM. One of the QDs maintains its polarization angle parallel to the CM one as Δ is varied. The other QD, which is the main focus of this paper, changes continuously its polarization angle from perpendicular to CM (at large Δ) to parallel to CM (at zero Δ). The polarization degree $P = (I_{MAX} - I_{MIN}) / (I_{MAX} + I_{MIN})$ remains high for all detunings. A qualitative explanation of this behaviour is given in terms of the detuning-dependent coupling of the QD exciton to the CM. The possible influence on our results of the selective emission enhancement for polarization parallel to CM due to the Purcell effect is also discussed.

2. Experimental details

The sample consists of a layer of randomly distributed self assembled InAs QDs grown by solid source molecular beam epitaxy. The QDs are located inside a 158 nm thick GaAs slab grown on top of a 500 nm thick AlGaAs sacrificial layer. Atomic force microscope images of the QDs before capping show a ring-like shape [10], which is not believed to be relevant for the present results. The ring-like shape of our QDs is relevant for Bohm-Aharonov-like experiments [11,12]. The only influence of the actual shape of our QDs could be the in-plane anisotropy leading to a preferential direction of the emitted light polarization, as it will be addressed in section 3. The QD surface density is $7.5 \times 10^9 \text{ cm}^{-2}$. The QD height is 2 nm and the lateral size is 50 nm on average. A PCM based on a triangular lattice of holes of 140 nm diameter with a lattice constant of 230 nm was patterned by e-beam lithography and dry etching. Comprehensive details on the membrane fabrication are given in Ref. [13]. The photonic bandgap provided by this lattice ranges from 736 nm to 952 nm. The cavity is formed by a missing hole in the photonic crystal and a slight inward shift of its nearest neighbours truncated holes (*calzone* cavity [14], see inset of Fig. 1). Air suspended membranes were realized by etching of the underlying sacrificial AlGaAs layer. The lowest energy cavity mode is split into two components with orthogonal linear polarizations separated by ~ 3.2 meV. Hereafter they will be designated as CMX and CMY modes (X corresponds to the long cavity diagonal, see inset of Fig. 1). The quality factors for CMX and

CMY are around 4000 and the mode volume is around $8 \times 10^{-3} \mu\text{m}^3$. Higher Q values (up to 10^4) have been reported in Ref. [14]. for similar cavities. Our smaller Q value is attributed to accidental deviations from the optimal hole size uniformity and the precise location, size and shape of the 6 innermost holes in the present cavity.

Photoluminescence (PL) spectra of single QDs were taken with a micro-PL setup producing a gaussian spot of $1.5 \mu\text{m}$ half width. The collection aperture was $\text{NA} = 0.5$ and the spectrometer slits were set to have a resolution of $100 \mu\text{eV}$. He-Ne and Ti-sapphire continuous lasers were used for non-resonant excitation and excitation resonant with the QD p-states respectively. The excitation intensities varied from $10 \mu\text{W}$ (HeNe) to 1mW (Ti-sapphire). The in-plane position of the light spot could be varied in 14nm steps by computer controlled step-motors. The detuning of the QD excitons from the cavity mode was varied either by changing the sample temperature in a continuous-flow He cryostat or by controlled in situ Xe thin film deposition [15]. The photon correlation measurements were done with a Hanbury-Brown and Twiss (HBT) interferometer. Two avalanche photodiodes with 30% efficiency at the QD emission energy (1.34eV) were used for coincidence detection. Their response time (0.5ns) was measured with 2ps pulses of a Ti-sapphire laser.

3. Results and discussion

Two selected quantum dots (QD1 and QD2 in the Fig. 1 inset) have been identified by maximizing their PL intensities as a function of the light spot position with an accuracy of 300nm . While QD2 can be excited both with X and Y polarizations, QD1 only emits under Y polarized resonant excitation. This can be due to the large geometrical asymmetry presented often by this kind of ring shaped QDs [16], which hinders the observation of the exciton fine-structure splitting. The PL spectra of Fig. 1 show the exciton emission of QD1 and QD2 together with CMX for X (black) and Y (red) polarization at 7K . One observes that the QD2 emission is linearly polarized parallel to CMX while QD1 polarization is mostly perpendicular to it for the actual detuning. We observed different polarization orientations also in the light emitted by QDs located far away from the cavity center. This indicates that the polarization direction is not determined by the crystal axes but rather by the shape and strain state of a specific QD.

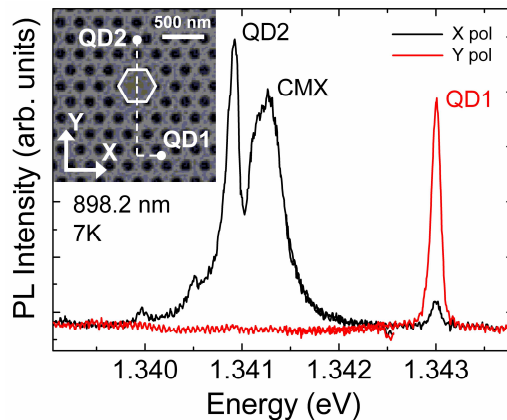


Fig. 1. (Color online) PL spectra of QD1, QD2 and CMX at two orthogonal polarizations (X-black and Y-red). Spectra were taken at 7K and with excitation resonant at the p states. QD1 emission is almost perpendicularly polarized to CMX and QD2 emission is parallel to it. Inset: SEM image of the microcavity with the location of QD1 and QD2.

The emission spectra of QD1 are presented in Fig. 2 for different temperatures [Fig. 2(a)–2(c)] and similar excitation conditions. The scales are the same for all detunings and polarizations. As the emission energy detuning between QD1 and CMX is varied upon raising the temperature, the PL spectra evolve both in intensity and polarization. The coupling between QD1 and CMX responsible for this intensity change is weak, as no energy

anticrossing is observed (the energy detuning Δ changes sign around 46K). The upper panels in Fig. 2(d)–2(f) display the corresponding polarization polar plots of QD1. While CMX maintains a 95% X polarization at all detunings, one observes a rotation of the polarization angle Φ of QD1 as a function of Δ . Its predominant Y polarization at large Δ progressively rotates towards X direction as Δ is decreased and changes sign for negative Δ [Fig. 2 (f)]. The polarization degree (red triangles in Fig. 3) varies between 0.6 and 0.8 in the detuning range studied, without showing a clear trend as a function of detuning. The polarization rotation is more clearly seen in Fig. 3, where the emission polarization angle of QD1 is presented as a function of detuning. A continuous change of Φ in the $+80^\circ/-80^\circ$ range is observed with sign reversal for negative detunings. To discard any possible thermal effect on the QD strain as the source of the polarization rotation, measurements at fixed temperature were included (blue squares) using Xe thin film controlled deposition to modify the CMX energy. The influence of CMY on the QD1 polarization angle is not expected to be important, as its detuning with respect to CMY changes from 2.6 to 5.1 meV in the temperature range corresponding to Fig. 3. The present result demonstrates the continuous control (including sign) of the polarization angle of a QD coupled to a cavity. Comparison with the result reported in Ref. [8] for micropillar cavities is not straightforward due to the different emission direction of QD photons and CM photons in micropillars already mentioned. Besides, only the polarization ratio $(I_X - I_Y)/(I_X + I_Y)$ was measured in Ref. [8], as a function of detuning, so that eventual changes in the polarization angle could not be observed.

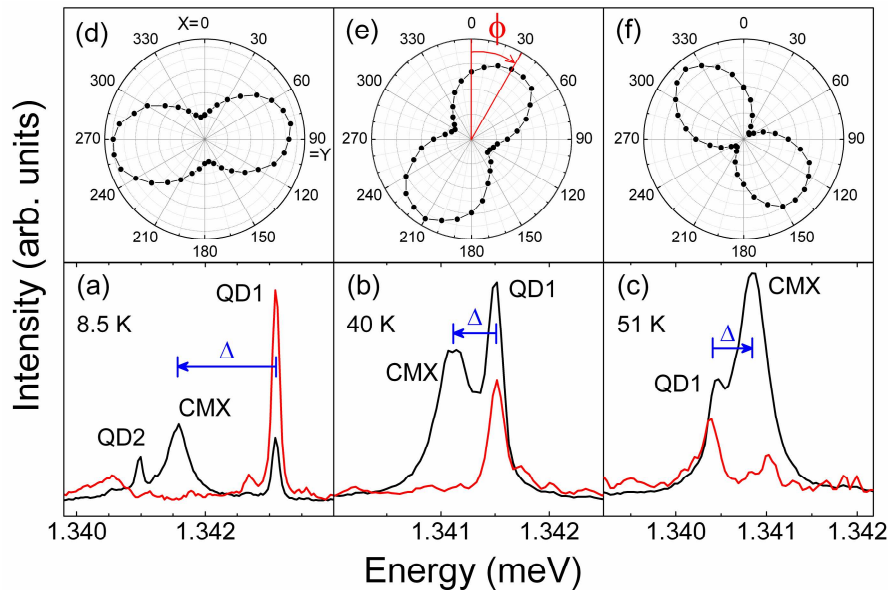


Fig. 2. (Color online) (a) (b) (c) Temperature dependent PL spectra of QD1, QD2 and CMX. Black (red) lines correspond to X (Y) polarization. Blue arrows indicate the sign of Δ . (d) (e) (f) QD1 polarization polar plots for the three temperatures shown below. A clear rotation of the polarization angle Φ is observed as the detuning is changed. $\Phi = 0^\circ$ (90°) corresponds to X (Y) polarization.

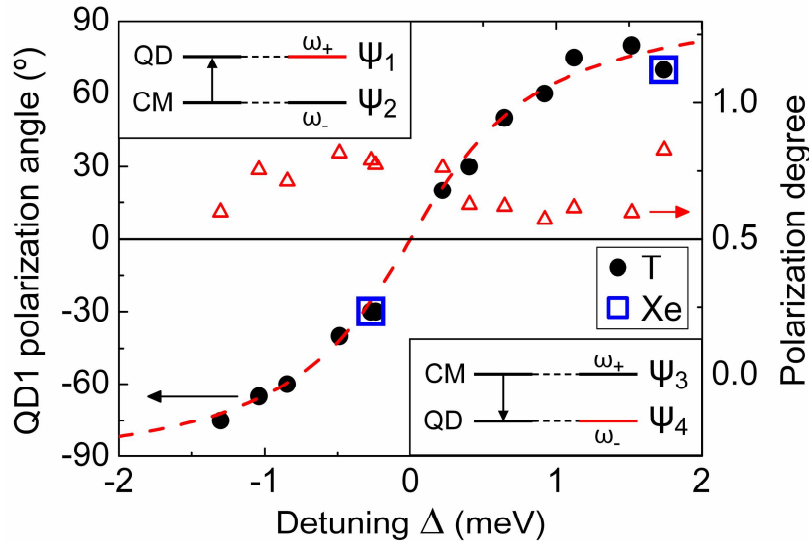


Fig. 3. (Color online) Polarization angle of QD1 emission recorded as a function of its detuning. The detuning was varied by changing the sample temperature (black dots). Blue squares correspond to measurements at the same temperature but changing the CM energy by using Xe thin-film deposition. The dashed line is a guide to the eye. Red triangles represent the polarization degree as a function of the detuning. Insets: Hybridized states for negative (top left) and positive (bottom right) detuning.

In contrast to QD1, the PL emission of QD2 (Fig. 4) preserves its X polarization even when its emission energy approaches that of the other ground state cavity mode CMY (black traces, 55K). This is shown in detail in the inset of Fig. 4 for higher excitation intensity. This result agrees with the one reported in Ref. [9], where a PCM was used. However, it differs from Ref. [8], where a QD inside a micropillar cavity emits X or Y polarized photons depending on which of the CMs is closer in energy to the QD. Again the different angular distribution of QD- and CM-photons can explain the difference with Ref. [8]. The different behaviour of QD1 and QD2 in our sample can be due to a difference in the intrinsic QD dipole orientation, which depends on QD anisotropy, strain, etc. and is specific of each QD. In this way, the polarization of the uncoupled (detuned) QD1 is polarized close to the Y direction, whereas the polarization of the uncoupled QD2 is already polarized along X, i.e. parallel to CMX. An additional effect which could also influence the QD polarization behavior would be related with the precise positions of the QDs with respect to the field pattern. The field strength distribution of the cavity modes has been calculated following Ref. [14], in an area of $300 \times 300 \mu\text{m}^2$ around the estimated QD locations (the uncertainty area). It undergoes strong variations, with minima close to zero, with a characteristic length scale of the order of the QD size, i.e., lower than the localization uncertainty of the QD. The field nodes and antinodes occur at different locations for CMX and CMY. Consequently, QD2 could accidentally lie in a CMY node, while the CMX field would be responsible for the intensity enhancement observed in Fig. 4.

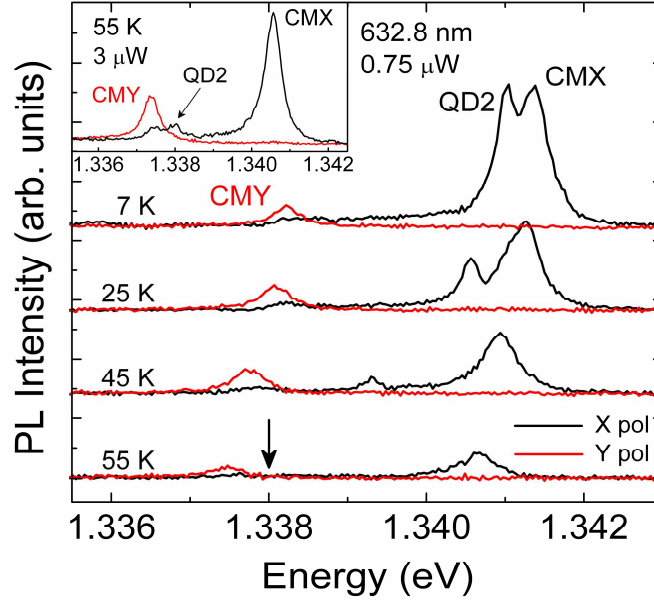


Fig. 4. (Color online) Temperature dependent PL spectra of QD2, CMX and CMY. Black (red) lines correspond to X (Y) polarization. The QD2 energy at 55K is marked by the arrow. Inset: PL spectra at 55K and higher excitation intensity. QD2 emission remains X-polarized even when its energy approaches the CMY.

The quantitative explanation of the polarization rotation found in QD1 would need a detailed knowledge of the coupling mechanism and the dynamics of the photon population in the coupled QD-CM system. Possible origins of the observed polarization rotation are: 1) the preferential enhancement of the QD emission polarized parallel to the cavity mode, due to Purcell effect, as Δ is reduced, and 2) the detuning-dependent hybridization of the QD and cavity states. The first one could have some influence on the variations observed in the polarization degree. Indeed the total emission, composed by the cavity-enhanced part (X polarized) and the “original” QD photons (Y polarized) would correspond to the superposition of two orthogonal emitting dipoles. This sum could produce a change in the polarization angle if the two dipoles are not strictly orthogonal. However considering the large difference in the polarization angle (at least 80°) as shown in Figs. 2 and 3, the resulting polarization degree should decrease strongly for any significant polarization rotation. This decrease is absent, as shown in Fig. 3, so that the preferential enhancement of the QD emission polarized parallel to the cavity mode has to be ruled out as the main origin of the observed polarization rotation. As for the second mechanism, it is worth mentioning that weak coupling is compatible with hybridization, as the eigenstates of the coherent Hamiltonian are linear combinations of QD and cavity state even if the dynamics of the system is determined by incoherent effects. In this context it is possible to give the following qualitative argument: hybridized states represented as linear combinations of the bare states of the CM (1,0) (parallel to X) and the QD (0,1) (parallel to Y) have the form:

$$\psi_1 = \frac{1}{\sqrt{1 + \left(\frac{g}{\omega_+}\right)^2}} \begin{pmatrix} 1 \\ g/\omega_+ \end{pmatrix} \quad \psi_2 = \frac{1}{\sqrt{1 + \left(\frac{g}{\omega_-}\right)^2}} \begin{pmatrix} g/\omega_- \\ 1 \end{pmatrix} \quad \text{for positive detuning}$$

and

$$\psi_3 = \frac{1}{\sqrt{1 + \left(\frac{g}{\omega_+}\right)^2}} \begin{pmatrix} \frac{g}{\omega_+} \\ 1 \end{pmatrix} \quad \psi_4 = \frac{1}{\sqrt{1 + \left(\frac{g}{\omega_-}\right)^2}} \begin{pmatrix} 1 \\ \frac{g}{\omega_-} \end{pmatrix} \quad \text{for negative detuning,}$$

where $g = g_{\text{vac}}\sqrt{n}$ is the strength of the effective coupling between the QD state and a CM state occupied with n photons; ω_{\pm} are the new emission frequencies: $\omega_{\pm} = \frac{\Delta}{2} \pm \sqrt{\frac{\Delta^2}{4} + g^2}$.

The QD state evolves into ψ_1 for $\Delta > 0$ and into ψ_4 for $\Delta < 0$, as shown in the insets of Fig. 3. As $\omega_+(\Delta) = -\omega_-(-\Delta)$, the sign of the polarization angle, given by ω_{\pm} , must follow the sign of Δ . This is consistent with the change in sign of Φ in Fig. 3, but does not explain the detailed dependence $\Phi(\Delta)$ found experimentally. A quantitative explanation of the trend shown in Fig. 3, as well as of the invariance of the CM polarization angle on detuning would require considering other factors, as a high photon occupation of the cavity mode. The present results show that, even in the weak coupling regime, the polarization of the emitted photons can be used for detecting the hybridization of QD and cavity states as a function of detuning.

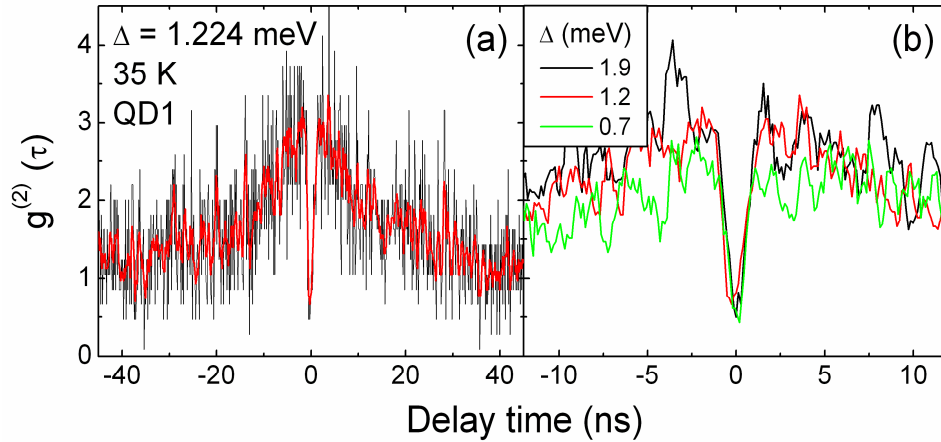


Fig. 5. (Color online) (a) Second order auto-correlation function of QD1 for Y polarization and 35 K (black trace). The red line is the smoothed curve of the experimental data. (b) Smoothed curves of $g^{(2)}(\tau)$ of the Y-polarized QD1 emission for different detunings showing similar antibunching peaks.

The photon auto-correlation function of QD1 is shown in Fig. 5(a) for large detuning (1.224 meV). The polarization collection was set perpendicular to the cavity mode to avoid the cavity background. The black trace corresponds to a time resolution of 128 ps. The red line is a smoothing of the experimental curve for better visualization. A narrow (~ 1.3 ns) antibunching peak is observed at zero delay time together with a broad bunching extending over ± 40 ns. The anti-bunching is indicative of single photon emission, while the bunching is attributed to the enhanced probability of QD recharge, after emitting a photon, by feeding from the cavity. Other QD being far away (3–4 μm) from the cavity center do not show any bunching. The antibunching is observed with no detectable changes for several detuning values [Fig. 5(b)] in the 0.7 to 1.9 meV detuning range. Below $\Delta = 0.3$ meV the antibunching is lost (not shown), probably due to the more efficient feeding from the cavity. The present results are encouraging for the development of single photon emitters with precise continuous control of the linear polarization orientation, although more detailed correlation measurements, together with a quantitative explanation of the observed polarization rotation, would be desirable for a complete understanding of this system.

4. Conclusions

In conclusion, we present experimental evidence of the precise control of the linear polarization emission angle of a selected QD coupled to a photonic crystal microcavity, by changing the energy detuning. Although a detailed explanation of the observed polarization rotation is not yet available, a plausibility argument in terms of QD and CM states mixing has been given. The intrinsic dipole orientation of the uncoupled QD and its precise location with respect to the cavity centre could play an important role in the polarization orientation dependence on the energy detuning.

Acknowledgements

The authors are indebted to E. Hu, R. Sabouni and D. Sanvitto for helpful discussions. This work has been supported by research contracts of the Spanish Ministry of Education Grants MAT2008-01555/NAN, Consolider CSD 2006-19 and Naninpho-QD TEC2008-06756-C03-01, and the Community of Madrid Grant Grant CAM (S2009/ESP-1503).